

Linear Quadratic Regulation Method for a Roll Yaw Coupled Supersonic Flight Vehicle

TAIN-SOU TSAY

Department of Aeronautical Engineering, National Formosa University, No.64,
 Wen-Hua Road, Huwei, Yunlin, TAIWAN

Abstract: In this literature, a linear quadratic regulation (LQR) method with controller reconfiguration and state observer is proposed for analyses and designs of a supersonic roll-yaw coupled flight control system. The flight control system of some specially shaped airframe can be decomposed into a Pitch Control System and a Roll-Yaw Coupled Control System. It can be designed separately, no need for three loops to be designed together. The design process is relatively simple, which is conducive to the design of flight control systems in large airspace. The proposed method for the considered system will give the good tracking characteristic at low frequencies and robustness at middle frequencies; simultaneously. All state variables are measurable and found controllers are all realizable either in analog or digital hardware.

Keywords: Flight Control System, Controller Realization, LQR method

Received: May 19, 2021. Revised: April 15, 2022. Accepted: May 14, 2022. Published: July 2, 2022.

1. Introduction

It is well known that the linear quadratic regulation (LQR) method provides good robust characteristics at middle frequencies [1, 2], if states of the considered system are all observable or measurable. State observer (or estimator) is usually used to find un-measurable states. But it will degrade the robust characteristic found by the LQR method. In another way, the performance of the system cannot be guaranteed at low frequencies; i.e., steady-state characteristics. In this literature, it will be seen that extra states from the integration of measurable states are introduced into the LQR procedure and reconfigured with proper positions of the summing of reference input commands. Then, the reconfigured system provides good tracking characteristics at low frequency. Since physical systems have low-pass characteristics, it needs not to pay much more attention to middle/high frequencies.

In general, only three body-axial angular rates (p, q, r) and two body-axial accelerations (a_{zacc}, a_{yacc}), those measured by rate gyros and accelerometers, are used as feedback signals for missile flight control systems [3, 4]. The angle of attack (α) and angle of sideslip (β) are two important states, but they are usually not observable for bad accuracy or slow datum updating rate. Such that state observer for α and β is generally needed. In the following sections, approximations ($\tilde{\alpha}, \tilde{\beta}$) of α and β are first used to replace α and β by other measurable states, and then perform the LQR method to find feedback control gains. Integrations of measurable states will be introduced also, and the controlled system will be reconfigured with constant gains, integrators, and reference input commands. It is similar to conventional command tracking control configurations [3, 4]. It will be seen that approximations ($\tilde{\alpha}, \tilde{\beta}$) of α and β keep robust properties of the LQR design after controllers realized by the proposed control configuration, and elements of

weighting matrices Q and R of LQR are closely related to bandwidths and crossover frequencies of inner loops. Thus one can easily meet designing specifications and reduce effects of hardware added to the considered system or use lead/lag compensatory to compensate effects of hardwires, especially for high frequencies, to keep considerable robustness obtained from LQR design.

The flight control system of some specially shaped vehicle can be divided into a Pitch Control System and a Roll-Yaw Coupled Control System; i.e., one single-input-single-output system and a two-input-two-output system. I can be designed separately, with no need for three loops to be designed together[5-7]. The design process is relatively simple, which is conducive to the design of flight control systems in large airspace.

2. Problem Formulation

For illustration, consider a linearized roll-yaw coupled system [8, 9] shown in Fig.1, and aerodynamic coefficients given in Appendix A [10, 11]. The differential equations of Fig.1 are in the form of

$$\dot{p} = L_p p + L_\beta \beta + L_{\dot{\beta}} \dot{\beta} + L_{\delta^*} \delta^* \quad (1)$$

$$\dot{\beta} = \tan \alpha^* p - r + M_B Y_\beta \beta + M_B Y_{\delta^*} \delta^* + M_B Y_{\dot{\beta}} \dot{\beta} \quad (2)$$

$$\dot{r} = N_r r + N_\beta \beta + N_{\delta^*} \delta^* + N_{\dot{\beta}} \dot{\beta} \quad (3)$$

$$a_{yacc} = Y_\beta \beta + Y_{\delta^*} \delta^* + Y_{\dot{\beta}} \dot{\beta} + L(N_r r + N_\beta \beta + N_{\delta^*} \delta^* + N_{\dot{\beta}} \dot{\beta}) \quad (4)$$

where p is the rolling angular rate, r is the yawing angular rate, a_{yacc} is the measured acceleration of the yawing channel, and α^* represents the trim condition of the angle of attack. Since the second term of Eq.(4) is much smaller than that of the first term, Eq.(2) can be approximated by the following equation

$$\dot{\tilde{\beta}} = \tan \alpha^* p - r + M_B a_{yacc} \quad (5)$$

where p , r and a_{yacc} are all measurable. Taking the integration of Eq. (5), one has

$$\tilde{\beta} = \tan \alpha^* \phi - \psi + M_B V_y \quad (6)$$

where $\phi = \int p dt$, $\psi = \int r dt$ and $V_y = \int a_{yacc} dt$. If β terms of

Eqs.(1)-(4) are replaced by $\tilde{\beta}$, then differential equations of the system can be rewritten as follows:

$$\dot{p} = L_p p + L_\beta (\tan \alpha^* \phi - \psi + M_B V_y) + L_{\delta p} \delta p + L_{\delta r} \delta r \quad (7)$$

$$\dot{\phi} = p \quad (8)$$

$$\dot{r} = N_r r + N_\beta (\tan \alpha^* \phi - \psi + M_B V_y) + N_{\delta r} \delta r + N_{\delta p} \delta p \quad (9)$$

$$\dot{\psi} = r \quad (10)$$

$$\dot{V}_y = (Y_\beta + LN_\beta) (\tan \alpha^* \phi - \psi + M_B V_y) + Y_{\delta r} \delta r + Y_{\delta p} \delta p + L(N_r r + N_{\delta p} \delta p + N_{\delta r} \delta r) \quad (11)$$

where $\dot{V}_y = a_{yacc}$. Then the state-space model for LQR is

$$\dot{X} = AX + Bu \quad (12a)$$

$$Y = CX + Du \quad (12b)$$

where $X = [p \ \phi \ r \ \psi \ V_y]^t$, $y = [\phi \ V_y]^t$ and $u = [\delta p \ \delta r]^t$.

The state variable p , r , and \dot{V}_y are all measurable; ϕ , ψ , and V_y are integrations of them. Such that all states are available for feedback controls. The cost function of the standard LQR [1,2] problem is in the form of

$$J = \int_{t_0}^{\infty} (X^t Q X + u^t R u) dt \quad (13)$$

Selecting proper weighting matrices Q and R , then found feedback controls are in the form of

$$u = -KX \quad (14)$$

where

$$K = \begin{bmatrix} K_{11} & K_{12} & K_{13} & K_{14} & K_{15} \\ K_{21} & K_{22} & K_{23} & K_{24} & K_{25} \end{bmatrix} \quad (15)$$

For single-input single-output (SISO) preliminary designs, K_{13} , K_{14} , K_{15} , K_{21} , and K_{22} of Eq.(15) will be equal to zeros for no aerodynamic and kinematical couplings; i.e., L_β , $N_{\delta p}$, $L_{\delta r}$, $Y_{\delta p}$, and $\tan \alpha^*$ are all set to be equal to zeros.

3. Controller Realization

The realization of feedback controls K of the LQR design of the roll-yaw coupled system is shown in Fig.2. It can be reconfigured with the following relationships of gains:

$$K_{ip} = K_{11}, K_{op} = K_{12} / K_{11},$$

$$K_{ir} = -K_{23}, W_{ir} = K_{24} / K_{23}, K_{or} = K_{25} / K_{24},$$

$$K_{or1} = -K_{13}, W_{ir1} = K_{14} / K_{13}, K_{ir1} = K_{15} / K_{14},$$

Fig. 3 shows the realization, in which K_{21} , K_{22} , K_{ir1} , W_{ir1} , and K_{or1} represent gains of cross-coupled controls; K_{sr} is the scaling factor for unity DC gain of yawing channel. This configuration is similar to the conventional configuration [3, 4] except that cross-coupled controls, and needs ten gains and three integrators for the roll-yaw coupled system, It needs another eight gains and two integrators for overall roll-pitch-yaw coupled system for couplings between pitching and yawing channels are usually much than those of between rolling and yawing channels or rolling and pitching channels [8, 9]. For SISO preliminary design, it is reduced to eight gains and three integrators needed for the roll-yaw uncoupled system. In the following designs, simplified roll-yaw coupled systems are considered for illustrating proposed design procedures.

4. Design Examples

Consider a roll-yaw coupled system with aerodynamic coefficients given in Appendix A, and perform design procedures stated in Sections II and III. The weighting matrices Q and R for the LQR method are selected properly for suitable bandwidths and crossover frequencies of inner loops of rolling and yawing channels. A possible choice is

$$R = \begin{bmatrix} 5000000 & 0 \\ 0 & 5000 \end{bmatrix} \quad (19)$$

$$Q = \begin{bmatrix} 1 & 0 & 0 & 0 & 0 \\ 0 & 20000 & 0 & 0 & 0 \\ 0 & 0 & 1000 & 0 & 0 \\ 0 & 0 & 0 & 1000000 & 0 \\ 0 & 0 & 0 & 0 & 20000 \end{bmatrix} \quad (20)$$

For fixed values of matrix R , values of (2, 2)th and (5,5)th elements of matrix Q affect bandwidths of the rolling channel and yawing channel; respectively, values of (1,1)th and (3,3)th elements of matrix Q affects crossover frequencies of inner loops of rolling and yawing channels; respectively, and value of (4,4)th element of matrix Q affects the behaviour of synthetic loop of the yawing channel [3, 4].

The design results of two sets of (α^*, β^*) are given in Appendix B, in which gives found feedback control gain matrices K , gains of realized control configuration, and

eigenvalues of $(A-BK)$'s and realized systems. From eigenvalues of $(A-BK)$'s and realized systems, it can be seen that Eq.(5) provides a good approximation for the angle of sideslip (β) . Figs. 4 and 5 show frequency responses of $(\alpha^*, \beta^*)=(12^\circ, 1^\circ)$ of only the rolling inner loop open and only the yawing inner loop open; respectively, in which give gain/phase margins and phase/gain crossover frequencies. Figs. 4 and 5 show that realized feedback control keeps robust properties of **LQR** designs; i.e., greater than 6dB and 60deg. Fig. 6 shows frequency responses of coupling from the yawing command a_{yc} to the rolling angular rate p . Note that the value of major aerodynamic cross-coupling term L_β [8,9] is about one-half of L_{δ_p} , conventional three SISO controls (i.e., without cross-coupled control) [3, 4] are not good enough for compensating effects of L_β to get suitable robustness and performance.

Figs. 7, 8, and 9 show frequency responses of the system with hardware and compensators. The compensators and models of hardware are given in Appendix C. The lead compensators PIC(S) and YIC(S) are used to compensate for the effects of hardware, especially for gain/phase at high frequencies. The gain/phase margins and phase/gain crossover frequencies of another set of $(\alpha^*, \beta^*) = (6^\circ, 1^\circ)$ are given in Table 1. It can be seen that compensated systems still have considerable robustness after the hardware is added. The low-frequency gain margin (LFGM) 0.39 shown in Fig.4 represents the compensated system has good property for against serious unstable aerodynamic coupling [8, 9].

5. Conclusions

In this literature, proposed design procedures have provided a way to apply the **LQR** method for supersonic missile flight control systems, and relations between feedback controls found by the **LQR** method and cross-coupled command tracking control configuration. The designing results have shown that proposed design procedures are powerful for the considered system and found controllers are all realizable.

References

[1]. B. D. Anderson and J. B. Moore, *Optimal Control: Linear Quadratic Methods*, Courier Corporation, Chelmsford, MA, USA, 2007.
 [2]. M. Athans and P. L. Falb, *Optimal Control: An Introduction to the Theory and its Applications*, Dover Publications, New York, NY, USA, 2013.
 [3]. F. W. Nesline and P. Zarchan, "Robust Instrumentation Configurations for Homing Missile Flight Control," *AIAA Guidance Control Conference, AIAA-Paper-80-1749*, 1980, pp. 209-219.
 [4]. F. W. Nesline and M. L. Nesline, "How Autopilot Requirements Constraint the Aerodynamic Design of Homing Missile," *American Control Conference*, 1984, pp. 716-730.
 [5]. T. S. Tsay, "Linear Quadratic Regulation Method for Supersonic Missile Flight Control System Design," *Journal of Aeronautics, Astronautics and Aviation, Series A*, Vol.38, No.3, pp.207-216, 2006.
 [6]. T. S. Tsay, "Decoupling the flight control system of a supersonic vehicle," *Aerospace Science and Technology*, Vol.11, pp.553-562, 2007.

[7]. T. S. Tsay, "Coupling Effects and Decoupling for Supersonic Flight Vehicle," *WSEAS Transactions on System and Control*, Vol.7, No.3, pp.108-117, 2012.
 [8]. Gerald Corning, "The Pitch-Yaw-Roll Coupling Problem of Guidance Missile at High Angle of Pitch (U)," *NAVWEPS-77383*, 1961.
 [9]. L. L. Crodvich and B. E. Amsler, "Pitch-Yaw-Roll Coupling," *AGARD-353*, 1961.
 [10]. W. J. Monta, "Supersonic Aerodynamic Characteristics of An Air-to-air Missile Configuration With Cruciform Wings and In-Line Tail Control," *NASA-TM-X-2666*, Langley Research Center, Hompton, Virginia, 1972.
 [11]. W. J. Monta, "Supersonic Aerodynamic Characteristics of A Sparrow III Type Missile Model With Wing Control and Comparison With Existing Tail-control Results," *NASA-TR-1078*, Langley Research Center, Hompton, Virginia, 1977.

APPENDIX A: Linearized Aerodynamic Models

The Linearized aerodynamic models of an air-to-air missile with skid-to-turn guidance for Mach number= 2.00 and Altitude=0.5Km with two sets of Angle of Attacks and sideslip (α^*, β^*) are given below:

A.1. $\alpha^* = 12.0^\circ, \beta^* = 1.00^\circ, VM=676.8m/s, L = 0.041,$
 $L_\beta = 8951.6, L_\alpha = 684.45, L_{\delta_p} = 15609, L_p = -3.8,$
 $L_{\delta_q} = 780.5, L_{\delta_r} = 780.45, Z_\alpha = -176.7, M_B = .0145,$
 $N_r = -2.23, N_\beta = 274.03, N_{\delta_r} = -599.7, N_{\delta_p} = -29.99,$
 $M_q = -2.23, M_\alpha = -739.53, M_{\delta_q} = -599.7, M_{\delta_p} = -29.99,$
 $Z_{\delta_q} = -30.61, Y_\beta = -95.853, Y_{\delta_r} = 30.61, Y_{\delta_p} = 0.000,$
 $\delta_r^* = 0.45^\circ, \delta_q^* = -11.33^\circ, a_y^* = -1.42G, a_z^* = -22.27G,$

A.2. $\alpha^* = 6.0^\circ, \beta^* = 1.00^\circ, VM=676.8m/s, L = 0.041,$
 $L_\beta = 4446.8, L_\alpha = 518.8, L_{\delta_p} = 15609, L_p = -3.8,$
 $L_{\delta_q} = 780.5, L_{\delta_r} = 780.45, Z_\alpha = -136.9, M_B = 0.0145,$
 $N_r = -2.23, N_\beta = 274.03, N_{\delta_r} = -599.7, N_{\delta_p} = -29.99,$
 $M_q = -2.23, M_\alpha = -490.96, M_{\delta_q} = -599.7, M_{\delta_p} = -29.99,$
 $Z_{\delta_q} = -30.61, Y_\beta = -95.853, Y_{\delta_r} = 30.61, Y_{\delta_p} = 0.000,$
 $\delta_r^* = 0.46^\circ, \delta_q^* = -11.33^\circ, a_y^* = -1.42G, a_z^* = -9.11G,$

Note that the terms with (*) represent trim conditions.

APPENDIX B: Feedback Gains and Eigenvalues

B.1. $(\alpha^*, \beta^*)=(12^\circ, 1^\circ)$

a. State feedback gain matrix

$$K = \begin{bmatrix} 0.0055 & 0.2686 & -0.0055 & -0.9023 & -0.0281 \\ 0.0046 & 0.1983 & -0.0837 & -2.1573 & -0.1220 \end{bmatrix}$$

b. Gains of realized control configuration

$$K_{op}=49.2175, \quad K_{ip}=0.0055,$$

$$K_{or}=0.0566, \quad W_{ir}=25.7823, \quad K_{ir}=0.0837,$$

$$K_{or1}=0.0311, \quad W_{ir1}=163.712, \quad K_{ir1}=0.0055,$$

c. Eigen values of (A-BK)

$$\begin{aligned} & -25.1788 \pm j 20.6231 \\ & -43.7590 \pm j 12.5597 \\ & -7.7944 \end{aligned}$$

d. Eigen values of the realized system with LQR gains

$$\begin{aligned} & -26.5175 \pm j 20.5905 \\ & -42.4246 \pm j 9.8443 \\ & -7.9494 \\ & 0.0000 \end{aligned}$$

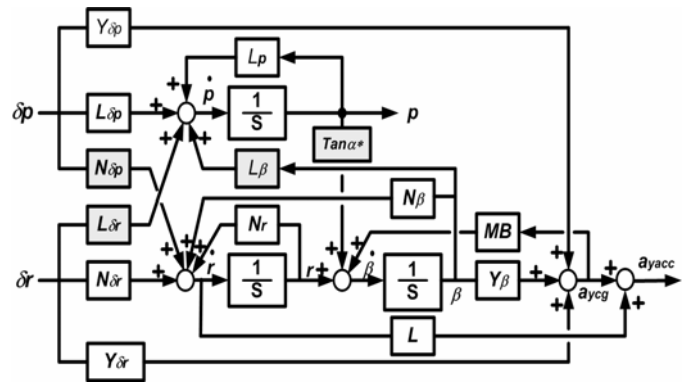


Fig.1. Linear Model of Roll-Yaw Coupled System.

APPENDIX C: Compensators and Hardware Models

1. Rolling inner loop compensator cascaded to K_{ip}

$$PIC(S) = \frac{S^2 / (2\pi 35)^2 + 2 \times 0.65S / (2\pi 35) + 1}{S^2 / (2\pi 65)^2 + 2 \times 0.80S / (2\pi 65) + 1}$$

2. Yawing inner loop compensator cascaded to K_{ir}

$$YIC(S) = \frac{S^2 / (2\pi 35)^2 + 2 \times 0.65S / (2\pi 35) + 1}{S^2 / (2\pi 55)^2 + 2 \times 0.85S / (2\pi 55) + 1}$$

3. Actuator model

$$CAS(S) = \frac{1}{S^2 / (2\pi 50)^2 + 2 \times 0.60S / (2\pi 50) + 1}$$

4. Rate gyro/accelerometer models

$$RG(S) = \frac{1}{S^2 / (2\pi 60)^2 + 2 \times 0.60S / (2\pi 60) + 1}$$

5. Inner loop low-pass filter body angular rate

$$LPFI(S) = \frac{1}{S / (2\pi 70) + 1}$$

6. Outer loop low-pass filter for acceleration

$$LPFO(S) = \frac{1}{S / (2\pi 30) + 1}$$

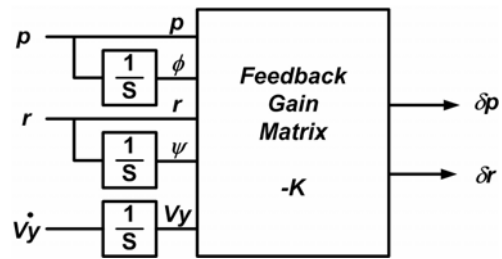


Fig.2. State Feedback Control Configuration.

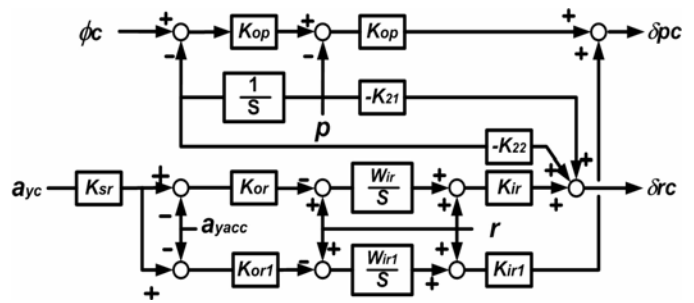


Fig.3. Realized Feedback Control Configuration.

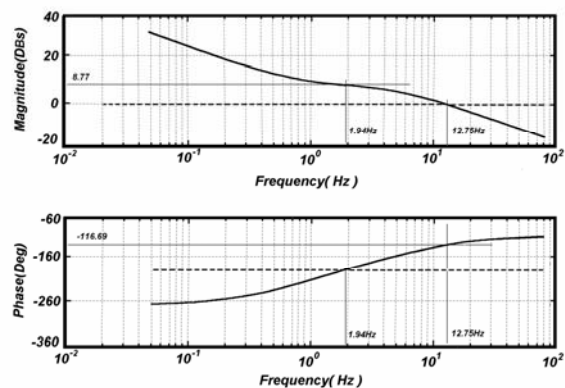


Fig.4. Frequency Responses of Only Rolling Inner Loop Open.

TABLE 1.

Gain/phase Margins and Phase/gain Crossover Frequencies.

Rolling Channel			Yawing Channel	
LFGM	HFGM	PM (°)	HFGM	PM (°)
0.23	3.36	42.2	6.67	60.1
1.83Hz	31.1 Hz	9.0Hz	16.5 Hz	9.5 Hz

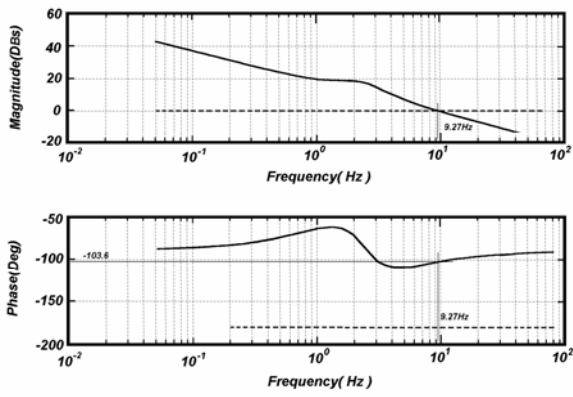


Fig.5. Frequency Responses of Only Yaw Inner Loop Open.

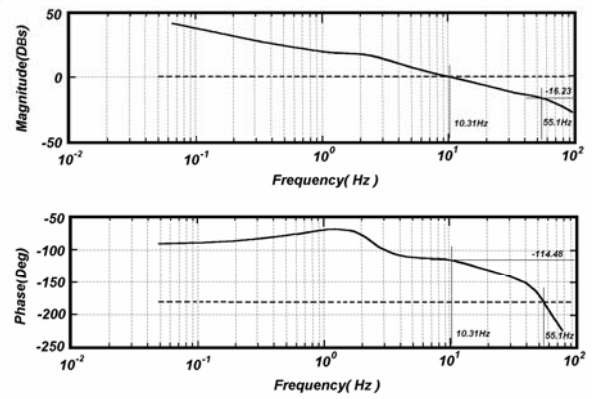


Fig.8. Frequency Responses of Only Yaw Inner Loop Open with Hardware.

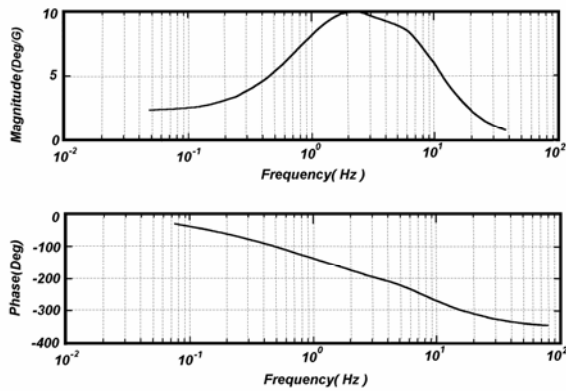


Fig. 6. Frequency Responses of Coupling Term P/a_{yc} .

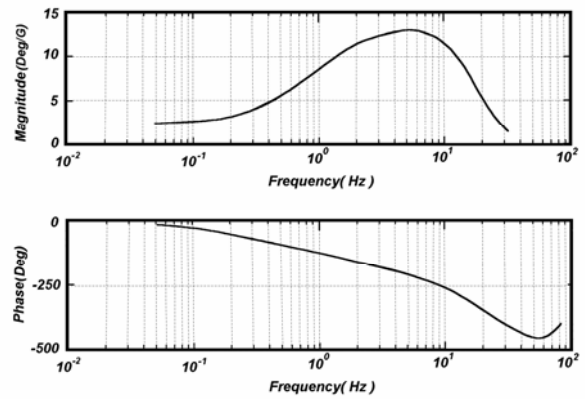


Fig. 9. Frequency Responses of Coupling Term P/a_{yc} with Hardware.

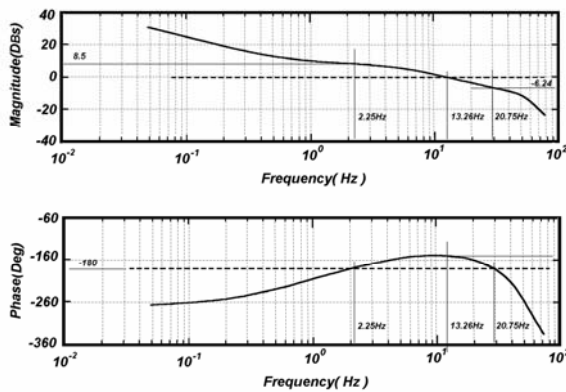


Fig.7. Frequency Responses of Only Rolling Inner Loop Open with Hardware.

**Creative Commons Attribution License 4.0
 (Attribution 4.0 International, CC BY 4.0)**

This article is published under the terms of the Creative Commons Attribution License 4.0

https://creativecommons.org/licenses/by/4.0/deed.en_US